A High Efficiency Rectenna Element using E-pHEMT Technology

C. Gómez, José A. García, A. Mediavilla, and A. Tazón.

Universidad de Cantabria. Dpto. Ing. Comunicaciones. Avda. Los Castros s/n, 39005 Santander, SPAIN.
Phone: (+34) 942 200918. Fax: (+34) 942 201488. Email: carmen@dicom.unican.es

***Abstract* — In this paper, a high-efficiency rectifying antenna (rectenna) element, based on a novel E-pHEMT detector, is proposed. The slightly positive threshold voltage in this technology, allows its use on resistive detectors without applying an auxiliary gate bias. Based on an adequate selection of the DC load resistor, as well as the drain and gate impedance conditions, the losses on the RF to DC conversion process are reduced. A high gain aperture coupled patch is finally designed, assuring optimum impedance values at the fundamental and second harmonic. Using a rectenna loading of *47Ω*, a *85.4%* measured overall efficiency is achieved.**

I. Introduction

The rectenna term was first proposed by Brown in [1]. It consists of a receiving antenna combined with a rectifying circuit, which converts RF or microwave power into useful DC power. The rectenna is a key element in wireless power transmission systems, deserving a lot of attention by the community during the last years.

Applications include, among others, the reception of a microwave beam sent to the earth by a geostationary solar power satellite [2], distributed DC powering of actuators [3], or DC supplying of RFID passive tags [4]. In all the cases, the RF to DC conversion efficiency is the figure to improve, over the range of incident power or output voltage of interest. Different solutions have been reported, mainly based on combining dipole or patch printed elements [5, 6] with diode detectors.

Different FET detector circuits have been proposed based on the R_{ds} nonlinearity [7]. However, these solutions have not found application in rectenna elements, mainly due to the need for using an auxiliary DC gate biasing voltage in order to obtain a good conversion result.

In this paper, the use of an Enhancement mode Pseudomorphic High Electron Mobility Transistor (E-pHEMT) in a rectenna is proposed. Due to its slightly positive threshold voltage, high conversion efficiency is possible for an unbiased detector topology.

First of all, a brief analysis of the E-pHEMT behavior as a detector is presented, based on an accurate characterization of the device main nonlinearity. Then, details on the design of a highly efficient detector circuit are discussed, paying particular attention to the DC load value, as well as to the gate and drain optimum impedance conditions. Finally, a rectenna element is proposed, combining the results of the referred detector with a high gain aperture coupled linearly polarized patch.

II. Simplified Analysis of the E-pHEMT Nonlinear Characteristics

E-pHEMT devices are normally-off FET transistors. A small positive gate to source voltage is required to form a conducting channel between drain and source terminals, as can be easily appreciated from the I/V characteristic of a typical device, plotted in Fig. 1.

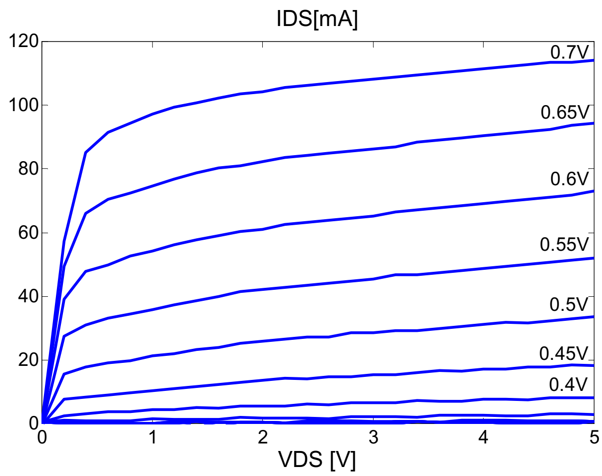

Fig. 1. $I_{DS}(V_{GS}, V_{DS})$ measured characteristic for an ATF-54143 E-pHEMT from Agilent Semiconductors.

Although care has to be taken with other nonlinear elements, the drain current source, $I_{ds}(V_{gs}, V_{ds})$, is the predominant factor determining the behavior of this kind of devices, while kept under normal operating conditions. A Taylor-series expansion of this nonlinearity up to the second order, around the biasing point, may help us introduce the particularities of an E-pHEMT behavior as a detector, at least when the applied RF excitation is small.

$$I_{ds}(V_{gs}, V_{ds}) = I_{DS}(V_{GS}, V_{DS}) + G_m v_{gs} + \\ + G_{ds} v_{ds} + G_{m2} v_{gs}^2 + G_{md} v_{gs} v_{ds} + G_{d2} v_{ds}^2 + \ldots \quad (1)$$

In (1), the transconductance G_m and the output conductance G_{ds} represent the I_{ds} partial derivatives with the V_{gs} and V_{ds} control voltages, respectively. On the other hand, G_{m2}, G_{md} and G_{d2} are the input, cross and output second order coefficients.

Using a FET device for RF to DC conversion implies working the transistor without applying any external DC drain to source bias [7]. In such a condition, considering the device as approximately unilateral, a small RF voltage applied between drain and source terminals, v_{ds}, would be efficiently converted to a DC drain to source current if the corresponding second order term were maximum.

$$G_{d2} = \frac{1}{2} \cdot \frac{\partial G_{ds}}{\partial V_{ds}} \bigg|_{V_{GS}, V_{DS}} = \max \tag{2}$$

For higher input RF excitations, a Taylor-series description up to the second order becomes inadequate. A better figure could be then provided by substituting the G_{d2} value at the initial condition, by the average value of the same coefficient all along the excursion imposed by the sinusoidal excitation, $\overline{G_{d2}(t)}_{RF}$.

The G_{d2} coefficient has a peak when a FET device is biased at the pinch-off or threshold voltage. Once the RF input power is increased, the maximum value of the $\overline{G_{d2}(t)}_{RF}$ coefficient widens, being usually shifted towards lower values.

In normal depletion type of devices, being the pinch-off voltage a negative quantity, a negative DC auxiliary voltage in gate terminal is always needed for assuring an optimum conversion. This fact makes depletion devices inappropriate for rectennas.

In an E-pHEMT device, however, the threshold voltage is slightly positive. Following the typical $\overline{G_{d2}(t)}_{RF}$ evolution with the input power, its maximum might be expected to appear at $V_{GS} = 0V$ for moderate power levels. This analysis was made for an ATF-54143, using the experimentally extracted G_{d2} Taylor-series term. In Fig. 2, the measured G_{d2} value and the computed $\overline{G_{d2}(t)}_{RF}$ behavior are plotted, as a function of V_{GS} for different input power levels. For low power levels, both terms coincide. For higher power values, the movement of the optimum conversion point from the threshold voltage to $V_{GS} = 0V$ is easily appreciated.

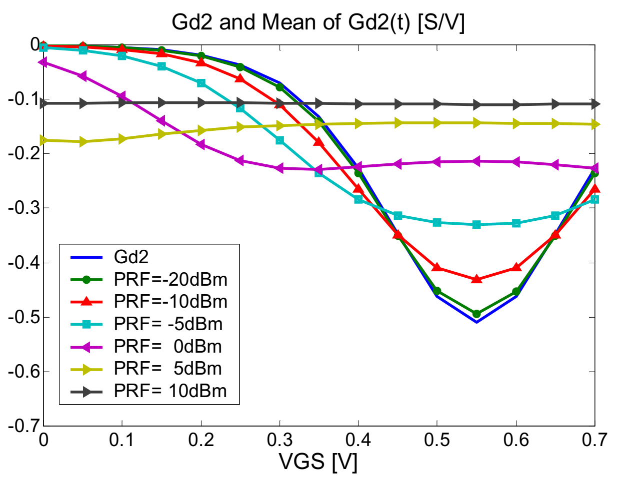

Fig. 2. Measured G_{d2} value and computed $\overline{G_{d2}(t)}_{RF}$ evolution with V_{GS} and P_{in} for $V_{DS} = 0\ V$.

III. Detector Design

Based on the above simplified analysis, an E-pHEMT detector was designed at the *900 MHz* band, using the topology shown in Fig. 3.

A. Drain and Gate Impedances

The role of the impedance condition on the conversion efficiency was first evaluated, both at drain and gate terminals.

A directional coupler was placed between the RF port and the detector to measure the reflected RF power. In this way, the influence of $Z_d(2fo)$, $Z_d(3fo)$ and $Z_g(fo)$ could be studied in equality of conditions through the use of the net conversion efficiency [6].

$$\eta_c = \frac{\text{DC output power}}{\text{incident RF power} - \text{reflected RF power}} \tag{3}$$

The drain impedance at the second harmonic was then adjusted, being significant its contribution to the efficiency figure. As it could be expected from previous diode works [5], the maximum was obtained for a small reactance value near a short-circuit. Such a reactance was implemented through a high Q series LC combination, see Fig. 3.

The effect of higher harmonics was also tested. The third harmonic drain impedance influence, however, was not as appreciable as the second one. As the best condition was found to be a very high reactive value, it was decided to use an open-circuit instead.

In the case of gate side, only the influence of the fundamental impedance was considerable. In this case, also a reactive value was found to be optimum, a value that resonates with the gate impedance of the transistor equivalent circuit. This reactance was assured through the use of a high Q coil, L_G. It is responsible for reflecting back all the incident power that could appear at gate terminal due to the feedback elements in the device equivalent circuit (R_s, C_{gd}).

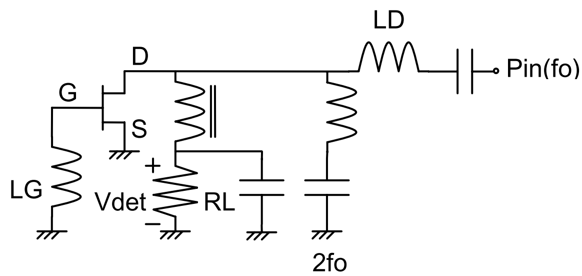

Fig. 3. Schematic of the E-pHEMT detector circuit.

B. DC Load Resistance

The optimum DC load value was also searched for, trying to maximize efficiency. The results for different load resistances, in the best range, are shown in Fig. 4.

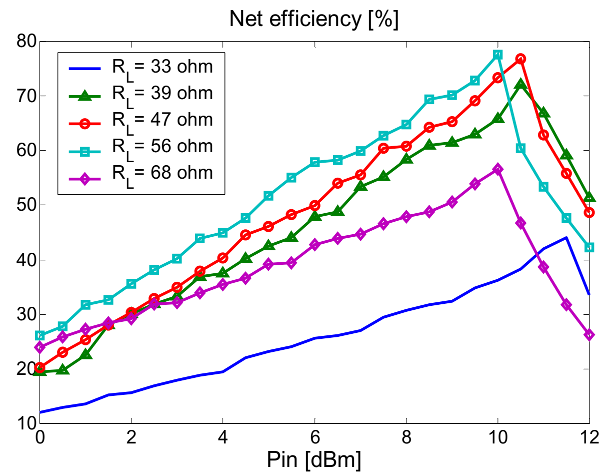

Fig. 4. Net efficiency for several R_L values.

The existence of an optimum value between *47 Ω* and *56 Ω* is evident. An increase of *Pin* above *10 dBm* resulted, however, in a reduction of the efficiency.

C. Impedance Matching.

Finally, with the optimum values for $Z_d(2fo)$, $Z_g(fo)$ and R_L, the input reflection coefficient was measured. A simple matching network was then added to transform to *50 Ω*, using a series coil at drain terminal L_D. Including this element, the maximum obtained overall efficiency, η_o, was of *73.2 %* at P_{in} = *10.5 dBm*, being this parameter defined as is shown in (4).

$$\eta_o = \frac{\text{DC output power}}{\text{incident RF power}} \tag{4}$$

This value could even be improved, if designing an antenna whose $Z_a(fo)$ were the conjugate of the detector impedance, while $Z_a(2fo)$ were resonant with the drain circuit. Thus, the losses in the employed lumped elements would be avoided.

IV. 900 MHz Antenna design

An ACMSA (aperture coupling microstrip antenna) [8] was selected for the rectenna design, due to its potential to work with active circuits. In the classical solution, the input impedance is controlled by the size, shape, and position of the aperture, while its excess reactance can be compensated for by varying the length of the open-circuited stub. Another stub was added in our design, so that the 2^{nd} harmonic impedance could be also adjusted.

Apart from assuring the appropriate load conditions, the antenna should provide a high gain. In this kind of radiator, this is possible when using a low permittivity material as radiator substrate. In order to use air permittivity, an inverted type of patch was employed [9].

The radiation from the detector may be also kept under control, thanks to the ground plane separating the circuit and the patch substrates.

The impedances at the fundamental and 2^{nd} harmonic were *47 + j5 Ω* and *2.5 + j28 Ω*, respectively, with a *|S11(fo)|* of *–25 dB* and a bandwidth of *45 MHz*. The gain was also measured, reaching a value of *9 dB*.

In Fig. 5, plots of the measured real and imaginary values for the designed antenna impedance are shown.

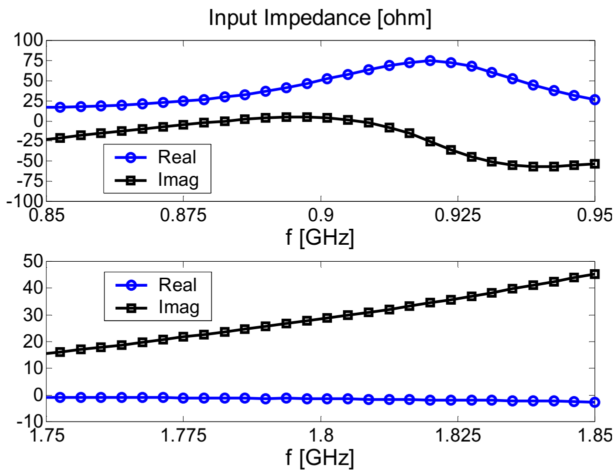

Fig. 5. Real and imaginary parts of the antenna impedance.

V. Rectenna Measurements

The rectenna (FET rectifier + antenna) was finally implemented. The detector circuit was inserted in the feed side of the previously designed antenna. The detector RF input port was located just in the place where the impedances at the fundamental and 2^{nd} harmonic frequencies were optimum for its conversion efficiency.

Fig. 6 shows a photograph of the rectenna, with a zoom made over the E-pHEMT detector part. In order to guarantee a minimum error in the efficiency computation, a port for having access to the received power was also included.

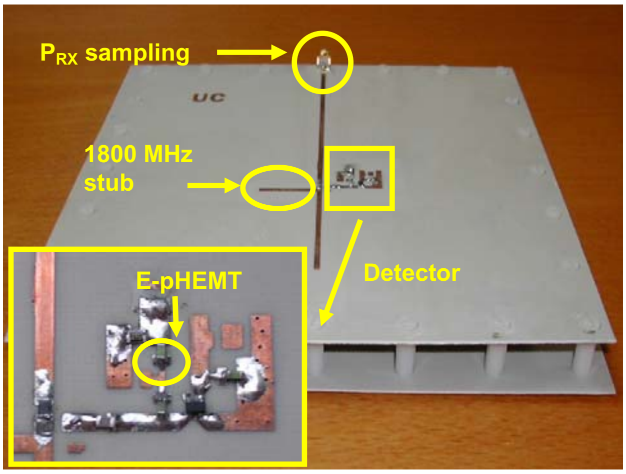

Fig. 6. Photograph of the E-pHEMT based rectenna.

In Fig. 7, the measured rectenna overall efficiency is plotted.

A highest value of *85.4%* overall efficiency was obtained at an input power level as low as *11.5 dBm*. This value is competitive with the figures obtained from diodes. Being able of obtaining a high efficiency for a small input power level, the power to be transmitted may be reduced or the operating distance may be increased.

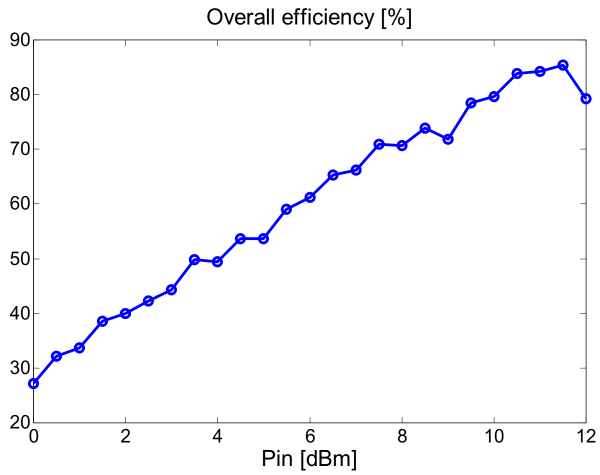

Fig. 7. Measured rectenna overall efficiency vs. the received power.

VI. Conclusion

A novel high efficiency rectifying antenna, using E-pHEMT technology, has been developed. The particularities of the device nonlinear behavior have been used to implement an unbiased transistor detector. A high gain patch has been designed, also providing the optimum impedance conditions for maximum conversion efficiency. The proposed rectenna provides a maximum efficiency of *85.4%* at *900 MHz* with an input power of *14.12 mW*.

Acknowledgement

The authors would like to thank the Spanish Ministry of Science and Technology (MCyT) by the financial support provided through project TIC 2002-04084-C03-03, as well as the European Commission assistance through TARGET Network of Excellence. J. A. Garcia is finally grateful to the Ramón y Cajal Program from MCyT.

References

[1] W. C. Brown et al., *U. S. Patent 3 434 678*, Mar. 25, 1969.

[2] W. C. Brown, "Status of the Microwave Power Transmission Components for the Solar Power Satellite," *IEEE Trans. Microwave Theory Tech.,* vol. MTT-29, no. 12, pp. 1319-1327, Dec. 1981.

[3] L. W. Epp, A. R. Khan, H. K. Smith, and R. P. Smith, "A compact dual-polarized 8.51-GHz rectenna for high voltage (50 V) actuator applications," *IEEE Trans. Microwave Theory Tech.,* vol. 48, no. 1, pp. 111-120, Jan. 2000.

[4] B. Strassner, and K. Chang, "Passive 5.8-GHz radio-frequency identification tag for monitoring oil drill pipe,", *IEEE Trans. Microwave Theory Tech.,* vol. 51, no. 2, pp. 356-363, Feb. 2003.

[5] T. Yoo, J. McSpadden, and K. Chang, "35 GHz rectenna implemented with a patch and a microstrip dipole antenna," *IEEE MTT-S Int. Microwave Symp*., pp. 345-348, June 1992.

[6] J. McSpadden, L. Fan, and K. Chang, "Design and experiments of a high-conversion-efficiency 5.8-GHz rectenna," *IEEE Trans. Microwave Theory Tech.,* vol. 46, no. 12, pp. 2053-2060, Dec. 1998.

[7] F. Carrez, and R. Stolle, "Novel low-cost, low-power modulator/demodulator using a single GaAs field effect transistor", *IEE Proc. Cicuits Devices Syst*., vol. 145, no. 3, pp. 165-169, June 1998.

[8] D. M. Pozar, "Microstrip Antenna Aperture Coupled to a Microstrip Line," *Elect. Lett.,* vol.21, no.2, pp. 49-50, 1985.

[9] J. F. Zurcher, "The SSFIP: a global concept for high-performance broadband planar antennas," Elect. Lett., vol. 24, no. 23, pp. 1433-1435, 1988.